Modeling and Optimization of EMS Maglev Tracks to Avoid Track-Induced Self-Excited Vibration

Danfeng Zhou, Kun Zhang, Yaozong Liu, and Jie Li
Maglev Engineering Center, National University of Defense Technology, P.O. Box 410073, Changsha, China
Danf.Zhou@gmail.com

ABSTRACT: For the EMS (Electromagnetic Suspension) maglev train, self-excited vibration in the levitation system may occur when the train is suspended above the track without moving. In this paper, the model of the steel track is firstly developed, and the principle underlying the self-excited vibration is then explored. It is found that the self-excited vibration in the levitation system is mainly caused by the flexibility of the steel track, and the self-excited vibration may occur only at some specified locations along the track. Furthermore, several tips of modifying the track structures, which are benefit for avoiding the self-excited vibration, are also presented. The work in this paper provides a reference for maglev track design.

1 INTRODUCTION

Recent achievements in the maglev train technology around the world indicate that the maglev systems are stepping into the commercial application stage (Yan 2008). For example, after the construction of the world's first commercial high speed maglev line in Shanghai, China is preparing to construct its first low speed commercial maglev route in Beijing – named as the S1 line – by 2012, adopting the EMS (Electromagnetic Suspension) technology.

The EMS maglev system utilizes controlled electromagnetic forces to neutralize the weight of the vehicle, thus the dynamic interaction between the vehicle and the guideway is quite complex. A problem caused by the interaction is the stability problem between the levitation system and the guideway, which appears in the form of a severe vibration in the track or the girder when the vehicle is moving at a very low speed. The test run of the CMS-03A and CMS-04 low speed maglev train on the Tangshan maglev test line have both encountered this problem. Different from the moving vehicle-guideway coupled vibration problem that has been widely studied for the wheel/rail system, the vibration in the track or the girder behaves as a self-excited vibration. Recently, Zhou et al. (2010) reviewed the study of the coupled vibration problems in the EMS maglev system, which showed that the self-excited vibration problem in the maglev system had not gained enough research attention. Since the maglev technology is stepping into the commercial application stage, this problem should be further investigated and be solved.

Recently, aiming at eliminating the self-excited vibration problem between the maglev train and the elevated girder, the model of the levitation system-girder coupled model has been investigated by Zhou et al. (2011a), and they found that the frequency of the girder plays an important role in the stability of the coupled vibration problem, and they suggested that the fundamental frequency of the girder should not be higher than the critical frequency of the levitation control system, and a virtual tuned mass damper was proposed to stabilize the coupled system. The self-excited vibration also occurs between the levitation system and the track frame. By using the finite element analysis software package, ANSYS, the coupled vibration problem between a maglev vehicle and a steel track frame was investigated by Li & Meng (2006). The modal shapes and frequencies of the track frame were computed, and it was concluded that the coupled vibration was caused by the second and third order modes of the frame

because the natural frequency of the secondary suspension system was coincident with these vertical modal frequencies of the frame. In addition, track-induced self-excited vibration always occurs when the vehicle is suspended at some specified locations along the track but without moving, and it appears that the track vibrates at a fixed frequency, thus making annoying noise. Fundamental work on this problem has also been undertaken by Zhou et al. (2011b,c). In (Zhou et al. 2011b), they have found that the flexibility of the steel track contributes to the occurrence of the self-excited vibration, and they tried to fix this problem by developing adaptive vibration control algorithms. In (Zhou et al. 2011c), the supporting conditions of the track have been taken into account, and they find that the supporting conditions play an important role in the stability of the electromagnet-track coupled system. The procedure of the stability analysis in (Zhou et al. 2011c) is also adopted in this paper to demonstrate the principle underlying the track-induced self-excited vibration.

However, in this paper, rather than to develop a vibration control algorithm, we try to find a method to avoid the self-excited vibration by modifying the current structure of the maglev track. To achieve this, the modal analysis technique is again employed to investigate the stability of the electromagnet-track coupled system, and the track model used in the analysis is further confirmed by finite element (FE) analysis method. At the end of this paper, several tips to ameliorate the structure of the track are proposed by using the finite element analysis. These tips are benefit for reducing the risk of the self-excited vibration problem.

2 MODELING OF THE TRACK

A segment of the low speed maglev track is shown in Figure 1, from which it can be seen that the track is composed of a pair of "F" shaped steel rails (referred to as the F-rail in the text below) and several sleepers. The lower layer of the maglev track, which is generally a concrete or a steel girder, is not shown in the figure, because the dynamic of the girder shows little effect on the occurrence of the track-induced self-excited vibration. Taking the vertical flexibility of the F-rail as well as the vertical and torsional flexibility of the sleepers into account, the track in each side can be modeled as a multiple supported beam with flexible support conditions, as shown in Figure 2.

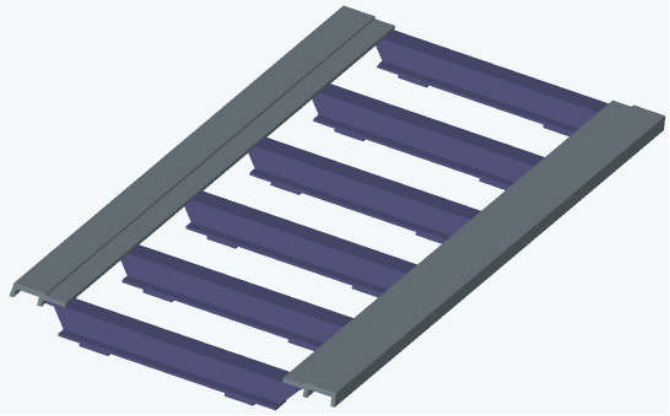

Figure 1. A segment of the low-speed maglev track.

In Figure 2, Ts_n = equivalent torsional stiffness of the n-th support; ks_n = equivalent vertical stiffness of the n-th support; L_n = span length of the n-th span; x_0 = location of the gap sensor on the track; l_0 = total length of the electromagnets; and f_0 = distributed electromagnetic force acting on the track.

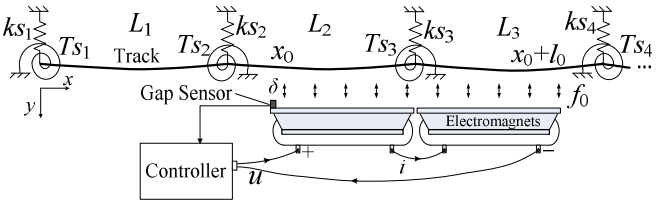

Figure 2. Simplified track model.

The vertical movement of the beam can be described as:

$$EI\frac{\partial^4 y(x,t)}{\partial x^4}+\rho\frac{\partial^2 y(x,t)}{\partial t^2}=f(x,t) \tag{1}$$

where EI and ρ = flexural rigidity and mass per unit length of the beam, respectively; $y(x,t)$ = vertical displacement of the beam; $f(x,t)$ = external force acting on the beam. For free vibration of the beam, $f(x,t) = 0$. Suppose $y(x,t) = \phi(x)\sin\omega t$, then Eq. (1) can be rearranged as

$$\frac{EI}{\rho}\frac{\partial^4\phi(x)}{\partial x^4}-\omega^2\phi(x)=0 \tag{2}$$

The form of Eq. (2) indicates that the solution for $\phi(x)$ can be described as a combination of the four types of trigonometric and exponential functions, and for the n-th span of the beam, it can be written as:

$$\phi_{(n)}(x)=C_{n1}\sin(\lambda x)+C_{n2}\cos(\lambda x)+C_{n3}\,\mathrm{sh}(\lambda x)+C_{n4}\,\mathrm{ch}(\lambda x) \tag{3}$$

where $\phi_{(n)}(x)$ = mode shape of the n-th span; λ = spatial frequency of the beam. Substituting Eq. (3) into Eq. (2), yields:

$$\omega^2 = EI\lambda^4 / \rho \tag{4}$$

The constants in Eq. (3) can be determined by the boundary conditions of the beam. The balance equations for the bending moment and share force of the beam at the left end can be separately written as:

$$EI\frac{\partial^2\phi_{(1)}(0)}{\partial x^2} = Ts_1\frac{\partial\phi_{(1)}(0)}{\partial x} \tag{5}$$

$$EI\frac{\partial^3\phi_{(1)}(0)}{\partial x^3} = -ks_1\phi_{(1)}(0) \tag{6}$$

At the intermediate supports, the balance equations for the bending moments and share forces are:

$$EI\frac{\partial^3\phi_{(n)}(x)}{\partial x^3}\bigg|_{x=L_n} = ks_{n+1}\phi_{(n)}(x)\big|_{x=L_n} + EI\frac{\partial^3\phi_{(n+1)}(x)}{\partial x^3}\bigg|_{x=0} \tag{7}$$

$$EI\frac{\partial^2\phi_{(n)}(x)}{\partial x^2}\bigg|_{x=L_n} = -Ts_{n+1}\frac{\partial\phi_{(n+1)}(x)}{\partial x}\bigg|_{x=0} + EI\frac{\partial^2\phi_{(n+1)}(x)}{\partial x^2}\bigg|_{x=0} \tag{8}$$

Similarly, at the right end of the beam, we have

$$EI\frac{\partial^2\phi_{(N)}(x)}{\partial x^2}\bigg|_{x=L_N} = -Ts_{N+1}\frac{\partial\phi_{(N)}(x)}{\partial x}\bigg|_{x=L_N} \tag{9}$$

$$EI\frac{\partial^3\phi_{(N)}(x)}{\partial x^3}\bigg|_{x=L_N} = ks_{N+1}\phi_{(N)}(x)\big|_{x=L_N} \tag{10}$$

where N = total number of spans.

In addition, the continuity of the displacement and slope at the intermediate supports require $\phi_{(n)}(L_n) = \phi_{(n+1)}(0)$, and $\phi'_{(n)}(L_n) = \phi'_{(n+1)}(0)$. Together with Eqs. (5) ~ (10), the unknown parameter λ and all the coefficients for Eq. (3) can be obtained. Generally, there are infinitely many solutions for λ, which can be obtained by numerical procedures.

The solution of Eq. (1) can be described as a combination of all the modal shapes obtained above, namely:

$$y(x,t) = \sum_{k=1}^{\infty} y_k(t)\phi_k(x) \tag{11}$$

Here, k = the order number of a mode; and $\phi_k(x)$ = the k-th order modal shape of the beam; $y_k(t)$ = displacement of the k-th order mode. Substituting Eq. (11) into Eq. (1), multiplying both sides of the resultant equation by $\phi_k(x)$, and integrating both sides from 0 to L, gives

$$\ddot{y}_k(t) + \omega_k^2 y_k(t) = \frac{F_k(t)}{M_k} \tag{12}$$

where

$$M_k = \rho\int_0^L \phi_k^2(x)\,\mathrm{d}x, \quad F_k(t) = \int_0^L f_0(x,t)\phi_k(x)\,\mathrm{d}x.$$

Here, the mode orthogonality condition for linear beams (Mikata 2008) has been applied, and L = total length of the beam. Equation (12) can be rearranged as

$$y_k(s) = \frac{F_k(s)}{\left(s^2+\omega_k^2\right)M_k} \tag{13}$$

The displacement of the k-th order vibration mode at x_0 is:

$$y_k(x_0,s) = \frac{F_k(s)\phi_k(x_0)}{\left(s^2+\omega_k^2\right)M_k} \tag{14}$$

Referring to Figure 2, it can be seen that the electromagnetic force is evenly distributed along the track, hence $f_0(t) = F_m(t)/l_0$; therefore,

$$F_k(s) = \frac{F_m(s)}{l_0}\begin{cases}\int_{x_0}^{x_0+l_0}\phi_k(x)\mathrm{d}x, & \text{if } x_0+l_0 \le L\\ \int_{x_0}^{L}\phi_k(x)\mathrm{d}x, & \text{if } x_0+l_0 > L\end{cases} \tag{15}$$

Then Eq. (13) can be rewritten as

$$y_k(x_0,s) = \frac{F_m(s)g_k\omega_k^2}{s^2+\omega_k^2} \tag{16}$$

where

$$g_k = \frac{\phi_k(x_0)}{l_0\omega_k^2 M_k}\begin{cases}\int_{x_0}^{x_0+l_0}\phi_k(x)\mathrm{d}x, & \text{if } x_0+l_0 \le L\\ \int_{x_0}^{L}\phi_k(x)\mathrm{d}x, & \text{if } x_0+l_0 > L\end{cases} \tag{17}$$

By analogy to a mass-spring system, Eq. (16) can be treated as a single degree-of-freedom (SDOF) resonator, and the coefficient g_k can be deemed as the flexibility of the k-th order vibration mode, which is named here as the mode gain of the k-th mode. Obviously, under the same excitement, lager g_k leads to larger amplitude of the vibration in the k-th order mode.

As a demonstration, the first three order modal shapes of a five span track (each span length equals 1.2 m) are shown in Figure 3. The vertical dashed lines in Figure 3 indicate the locations of the supports, while the horizontal dashed line indicates the original shape of the beam without vibration. Additionally, the corresponding mode gains for these modes are shown in Figure 4. In the calculation, the track parameters are chosen as: l_0 = 1.32 m, ρ = 121 kg/m, EI = 1.6×10^6 N m^2, ks_n = 8×10^7 N/m, and Ts_n = 4.5×10^5 Nm/rad.

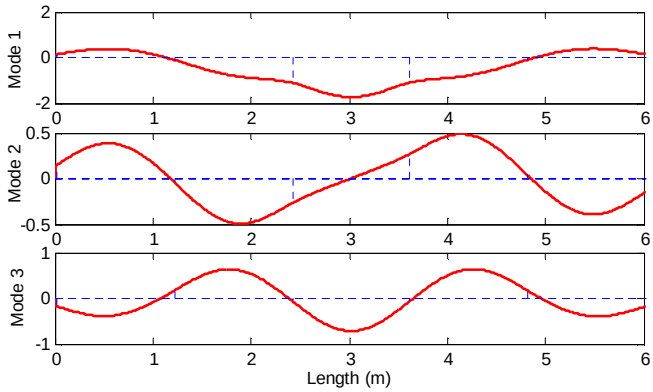

Figure 3. The first three order modal shapes of the track.

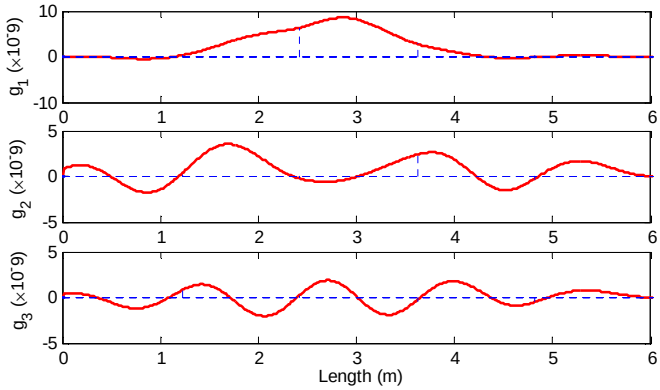

Figure 4. Mode gains for the first three order vibration modes.

Figure 4 indicate that the mode gains for the for the first three order vibration modes of the track appear to be negative at some locations along the track. It has been shown in (Zhou et al. 2011c) that this can be a factor which may destabilize the electromagnet-track coupled system and may cause the self-excited vibration to occur. This can be qualitatively interpreted by referring to Eq. (16), where the sign of g_k dominates the relative direction of the electromagnetic force, F_m, and the displacement of the track, y_k. Apparently, if g_k is positive, the response of y_k is similar to that of an SDOF resonator; however, if g_k is negative, the response of y_k is in-phase opposite to that of an SDOF resonator, and in this case, the stability condition of the coupled system may be breached and self-excited vibration may occur. This explains why in practice the occurrence of the track-induced self-excited vibration highly depends on the relative location of the electromagnet along a track.

To verify the reliability of the track model established above, the finite element analysis method is employed to calculate the modal shapes and modal frequencies of the track that has been shown in Figure 1. Here, the material of the track is chosen as the Q235 steel. The result of the FE method shows a good agreement with the theoretical analysis, and all the modal shapes shown in Figure 3 can also be found in the FE result. For example, the first and the second order modal shapes of the track obtained by the FE method are shown in Figure 5 and Figure 6, respectively. It can be seen that the vertical displacement of the F-rail is almost identical to the curves shown in Figure 3. Table 1 shows the comparison of the modal frequencies obtained by the two methods for the first three order vibration modes.

Table 1. Modal frequencies of the track.

Mode order	Theoretical result (Hz)	FE method (Hz)
1	111.3	111.2
2	116.0	120.6
3	124.7	125.5

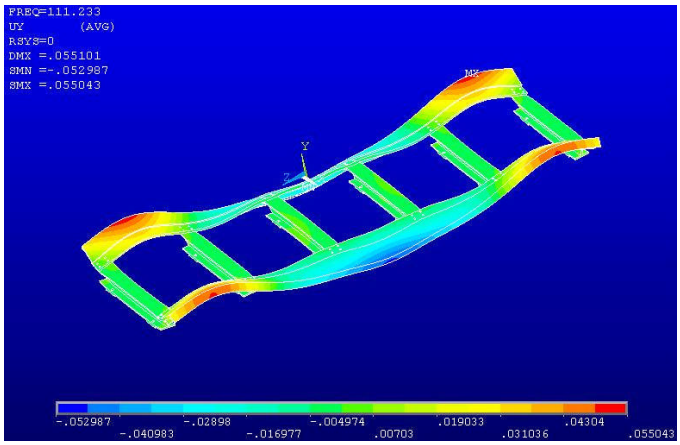

Figure 5. The first order modal shape of the track obtained by the FE method.

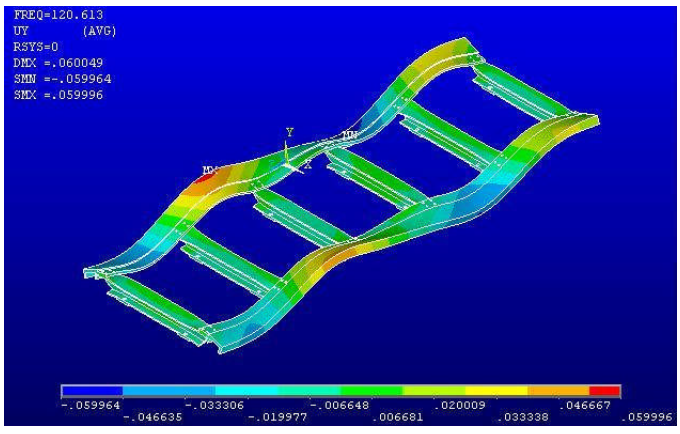

Figure 6. The second order modal shape of the track obtained by the FE method.

However, the FE result also includes some other modal shapes that cannot be obtained by the theoretical analysis; it is mainly because the modal shapes obtained by the FE method contains not only the vertical deformation of the track, but also the torsional deformation of the F-rail around its contact points with the sleepers.

3 OPTIMIZATION OF THE TRACK

From Eq. (17) it can be seen that the mode gain is inversely proportional to the square of the modal frequencies and M_k; therefore, to increase the stability of the electromagnet-track coupled system, the following procedures can be undertook to optimize the structure of the track.

3.1 Increase the thickness of the F-rail.

From Figure 5 it can be seen that the major deformation comes from the vertical and torsional deformation of the F-rails. Hence, increasing the stiffness of the F-rail would benefit the stability of the coupled system. The FE analysis shows that a 30% increase of the thickness of the plate which contacts with the supports in the F-rail can significantly increase the natural frequencies of the track. In the other hand, this method can also increase the mass of the F-rail, which can also increase the value of M_k, which in turn, decreases g_k.

Yet it is obvious that this method is uneconomical. Another problem is, once the structure design of the maglev bogie has finished, it is not always convenient to modify the dimensions of the F-rail, because the space inside the electromagnets and the linear motors is quite limited.

3.2 Increase the thickness of the sleepers.

Figures 5-6 also indicate that the stiffness of the sleepers play an important role in the modal shapes of the track. Insufficient stiffness of the sleepers would lead to lower natural frequencies of the track and more severe torsional deformation of the F-rail, thereby degrades the stability of the coupled system. The FE method shows that by increasing the thickness of the vertical plate in the sleeper from 20 mm to 40 mm can greatly increase the vertical stiffness of the track, which increases the modal frequencies of the track, as the comparison shown in Table 2.

Table 2. Modal frequencies of the original and the reinforced track.

Mode order	Original track(Hz)	Reinforced track (Hz)
1	111.2	123.9
2	120.6	132.4
3	125.5	137.9

In addition, the increase of the thickness of the sleepers also increases M_k, which is also beneficial to the stability of the coupled system.

An alternative way to increase the natural frequencies of the track is to increase the thickness of the upper plate of the sleeper. For example, increasing the thickness of the upper plate from 18 mm to 30 mm would lead to an increase of the modal frequencies, as shown in Table 3. This method, although not so efficient as the previous method, significantly increases the torsional stiffness of the sleepers, thus it is beneficial to the torsional stability of the coupled system.

Table 3. Modal frequencies of the original and the reinforced track.

Mode order	Original track(Hz)	Reinforced track (Hz)
1	111.2	117.7
2	120.6	126.2
3	125.5	130.6

3.3 Adding brace bars to the sleepers.

The methods proposed above have a common defect: they significantly increase the total cost of the whole project. Yet alternative ways to achieve the target of increasing the stiffness of the sleepers in the presence of not increasing too much cost can also be found. For example, this object can be achieved by adding several brace bars to the sleepers, as shown in Figure 7.

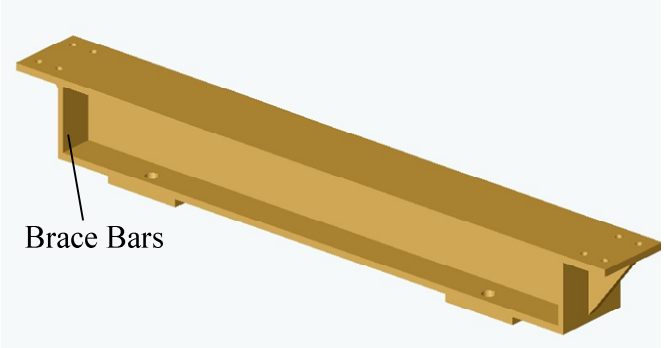

Figure 7. Reinforced sleeper by adding extra brace bars.

The FE analysis shows that this scheme can easily achieve a satisfactory increase of the modal frequencies by adding four 15 mm-thick brace bars at each end of a sleeper. Table 4 lists the first three order modes of the reinforced track. It can be seen that by using the optimized structure shown in Figure 6, the increases of the modal frequencies are prominent, especially for the higher order modal frequencies.

Table 4. Modal frequencies of the original and the reinforced track.

Mode order	Original track(Hz)	Reinforced track (Hz)
1	111.2	116.3
2	120.6	130.8
3	125.5	143.1

For comparison, Table 5 shows the relative mass increase of the sleeper when using the optimization methods discussed above. Apparently, the last method is the best choice in the practical application, because it not only shows equivalent or even better performance than the other methods, but it is also cost efficient.

Table 5. Mass increase when using different methods.

Thickened upper plate (%)	Thickened vertical plate (%)	Using brace bars (%)
20.4	28.8	4.7

4 CONCLUSION

In this paper, taking the stiffness of the F-rail and the sleepers into account, the dynamic model of the low speed maglev track has been established by simplifying the steel track as a multiple span beam with flexible supports, and on this basis, the principle underlying the track-induced self-excited vibration has also been discussed. The assumptions in the track modeling are validated by the finite element analysis technique, which proofs that the assumption of the multiple span beam is reasonable in the analysis of the electromagnet-track coupled system. A concept of modal gain is adopted in this paper to demonstrate the effect of the modal shapes to the stability of the coupled system, and it has been shown that negative modal gain is a major factor which may lead to the self-excited vibration, and that the flexibility of the track plays a vital role in the stability of the coupled system. At the end of this paper, aiming at increasing the stiffness of the track, several track optimization methods have been proposed, which showed that adding extra brace bars to the sleepers is the best way to achieve the object. The study in this paper provides an effective reference for maglev track design.

5 REFERENCES

Yan L.G. 2008. Development and application of the maglev transportation system. *IEEE Transactions on Applied Superconductivity* 18(2): 92–99.

Zhou D.F., Hansen C.H., Li J., Chang W.S. 2010. Review of coupled vibration problems in EMS maglev vehicles. *International Journal of Acoustics and Vibration* 15(1): 10−23.

Zhou D.F., Hansen C.H. & Li J. 2011a. Suppression of maglev vehicle-girder self-excited vibration using a virtual tuned mass damper. *Journal of Sound and Vibration* 330: 883−901.

Zhou D.F., Li J. & Hansen C.H. 2011b. Suppression of maglev track-induced self-excited vibration using an adaptive cancellation algorithm. *Applied Mechanics and Materials* 44-47: 586−590.

Zhou D.F., Li J. & Zhang K. 2011c. An adaptive control method to suppress the maglev track-induced self-excited vibration. *Proc. 2011 International Conference on Consumer Electronics, Communications and Networks, April 2011*. Xianning: China.

Li L. & Meng G. 2006. Analysis of the coupled vibration between the maglev vehicle and the steel track frame during levitating up and down. *Journal of Vibration and Shock* 25(6): 46−48. (in Chinese)

Mikata Y. 2008. Orthogonality condition for a multi-span beam, and its application to transient vibration of a two-span beam, *Journal of Sound and Vibration* 314: 851−866.